Journal of Atmospheric and Solar-Terrestrial Physics 80 (2012) 111–123

Contents lists available at SciVerse ScienceDirect

Journal of Atmospheric and Solar-Terrestrial Physics

journal homepage: www.elsevier.com/locate/jastp

Solar and interplanetary triggers of the largest *Dst* variations of the solar cycle 23

Y. Cerrato [a], E. Saiz [a], C. Cid [a,*], W.D. Gonzalez [b], J. Palacios [c]

[a] Space Research Group – Space Weather, Departamento de Física, Universidad de Alcalá, Spain
[b] Instituto Nacional de Pesquisas Espaciais, Brazil
[c] Image Processing Laboratory, Universidad de Valencia, Spain

ARTICLE INFO

Article history:
Received 24 March 2010
Received in revised form
7 September 2011
Accepted 10 September 2011
Available online 20 September 2011

Keywords:
Dst index
Geomagnetic storm
Halo CME
Interplanetary disturbances

ABSTRACT

We present the results of an investigation from the Sun to the Earth of the sequence of events that caused major *Dst* decreases ($\Delta Dst \leq -100$ nT during 1 h) that occurred during 1996–2005. These events are expected to be better related to geomagnetic induced current (GIC) events than those events where any geomagnetic index is far from its quiet time value. At least one full halo CME with a speed on the plane of sky above 900 km/s participates in every studied event. The seven events were triggered by interplanetary signatures, which arise as a consequence of interaction among different solar ejections. The interaction arises at different stages from the solar surface, between segments of a filament, to the interplanetary medium, appearing as ejecta or multiple-magnetic clouds (MultiMCs). In other cases, shock waves overtake or compress previous ICMEs and at other times the interaction also appears between magnetic clouds (MCs) and streams.

1. Introduction

As solar wind disturbances from solar ejections interact with the Earth's magnetic field, large electric currents arise in the terrestrial magnetosphere, ionosphere and in the conducting ground. As a consequence, geomagnetic induced currents (GIC) also arise in technological systems, leading to failures in the normal operation of the systems. A large number of studies have been devoted to the understanding of the solar and interplanetary sources of these geomagnetic events (e.g. Gonzalez et al., 1999, 2007; Burlaga et al., 2001; Cid et al., 2004; Huttunen et al., 2005; Zhang et al., 2007; Echer et al., 2008a, 2008b; Lario et al., 2008).

Different geomagnetic indices, such as *Dst*, *AE*, or *PC* indices, have been established to quantify the geomagnetic disturbance at different latitudes at the terrestrial surface. Other indices, such as *Kp* or *am*, have been considered as proxies of the planetary disturbance. However, the *Dst* index has been used extensively as the proxy for the intensity of the overall disturbance (Gonzalez et al., 1994). Choosing the minimum value reached by the *Dst* index, or Dst_{peak}, as a proxy for the severity of the storm, some failures in technological systems could pass as not related to space weather, even if they were. As an example, we can cite the papers by Belov et al. (2007) and Eroshenko et al. (2010) about the relationship between the response of the Signalization, Centralization and Blockage (SCB) system in the high-latitude parts of Russian railways and severe geomagnetic storms. In Table 1 of Eroshenko et al. (2010) a list of magnetic storms appears where failures occurred in the automatic railway system SCB. For most of these events, the *Dst* index peaked below −200 nT or even below −400 nT, but failures were also registered on January 21, 2005, when *Dst* reached only −105 nT, or on April 8, 2001, when *Dst* just reached −51 nT.

Koen and Gaunt (2002) conclude that the *K*-index and NOAA classification of storm severity are not directly related to the magnitude of GICs in networks. They suggest that an improved index for representing the severity of storms and, ideally, issuing warnings, should include the magnitude of the magnetic field variation with time, which determines the electric field available to drive GICs. Therefore, choosing the value for the maximum disturbance as measured by other indices instead of Dst_{peak} does not solve the problem. On this line Vodyannikov et al. (2006) conclude that unwanted consequences could arise in power systems during long periods with the time derivative of the geomagnetic field horizontal component exceeding 30 nT/min. Therefore, the reason for the failures related to GICs should be analyzed, not only looking how much the terrestrial magnetic field varies but also looking how fast it changes.

In this scenario, the aim of this paper is to address the solar and interplanetary sources of the largest variations of the *Dst* index along the last solar cycle. The understanding of the triggers of large decreases in *Dst* can also be considered an advance related to the fact that we are dealing with the largest way of

* Corresponding author. Tel.: +34918856424; fax: +34918854952.
E-mail address: yolanda.cerrato@uah.es (C. Cid).

1364-6826/$ - see front matter © 2011 Elsevier Ltd. All rights reserved.
doi:10.1016/j.jastp.2011.09.001

Table 1
List of events of solar cycle 23 with $dDst/dt \leq -100$ nT/hour arranged by the value of the $dDst/dt$, calculated as $Dst_{t+1\,hour} - Dst_t$. The values in columns 2–5 (year, month, day, hour) corresponds to t. The minimum values reached in $dDst/dt$ and Dst, for every event, appear in columns 5 and 6, respectively. Column 7 shows interplanetary triggers for the large $dDst/dt$ events (see text for more details).

Event	$dDst/dt \leq -100$ nT date				$(dDst/dt)_{min}$ (nT/hour)	Dst_{peak} (nT)	Trigger of $dDst/dt$
	yyyy	mm	dd	hh			
1	2005	05	15	06	−170	−263	Compressed MC by a second MC
2	2001	11	06	02	−168	−292	Overtaking shock through an ICME
3	2005	08	24	09	−158	−216	MC compressed by a fast stream
4	2001	03	31	04	−148	−387	Sheath and 1st MC of a Multi-MC
5	2000	07	15	19	−137	−301	Sheath compressed by succesive or merging of shock waves
6	2000	09	17	21	−110	−201	Sheath of a complex ejecta
7	2003	11	20	16	−100	−422	Possible interaction between segments of a filament

disturbance of the terrestrial magnetosphere. In Section 2 we set the criterion to select the events to be studied and in Section 3 we carry out a detailed analysis about the interplanetary causes and also provide an identification of solar sources that could have triggered the events. Finally, our conclusions are given in Section 4.

2. Events selection

As previously pointed out by Koen and Gaunt (2002), GIC events are related to the magnitude of the magnetic field intensity variation with time at the terrestrial surface. Previous studies computed the time derivative of the magnetic field horizontal component (dH/dt) using the highest resolution data available from local magnetometers. However, there is not any systematic study about the resolution of magnetic field data that should be used in order to calculate dH/dt for purposes of space weather forecasting.

Figures 6–9 of Eroshenko et al. (2010) show Kp and Dst indices for the geomagnetically disturbed periods analyzed in the paper, together with the times of the observed anomalies. Just at first glance of those figures one can observe that Dst (which is an hourly index) showed fast drops at that time. Specifically, all failures in the SCB system, from Table 1 of Eroshenko et al. (2010), took place when the time derivative of Dst calculated as $Dst_{t+1\,h} - Dst_t$, was below −50 nT/h.

There were 31 events where $dDst/dt \leq -50$ nT/h during solar cycle 23 (Saiz et al., 2008). This number of events is too large to perform a detailed study of the solar and interplanetary drivers, which were related to the large time derivative of Dst and therefore to the probability of a GIC event. Therefore, we are undertaking this study by choosing a threshold of $dDst/dt = -100$ nT/h, thus reducing in this way the number of events to be carefully analyzed. Based on this criterion, we analyze seven events that are listed in Table 1. This table shows event number, the date (year, month, day, hour) where the minimum hourly variation $(dDst/dt)_{min}$ takes place, the corresponding Dst_{peak} value and the associated interplanetary candidate for the large Dst variation.

Five out of the seven analyzed events are superstoms, with peak Dst reaching less than −250 nT (Echer et al., 2008a). The peak Dst indices for the other two events were below −200 nT. Therefore, all of them have been previously analyzed in the literature (e.g. Echer et al., 2008a; Cid et al., 2008; Gopalswamy et al., 2007; Zhang et al., 2007; Xie et al., 2006; Wang, 2007). However, the aim of this work is to highlight the common features that may have triggered the largest hourly variation of the Dst index.

Throughout this paper, we review the literature related to the seven selected events, paying special attention to the possible solar and interplanetary events related to the large and sharp decrease of the Dst index. For that task we use the LASCO CME list (http://lasco-www.nrl.navy.mil/cmelist.html), the Hα and X-ray flare events from the National Geophysical Data Center (http://www.ngdc.noaa.gov/stp/ SOLAR/flareint.html), and the solar wind magnetic field and plasma data shifted to the Earth's Bow Shock Nose from OMNIweb database (http://omniweb.gsfc.nasa.gov/ow_min.html) with 1 min resolution. The seven events are described in order of decreasing absolute value of the $dDst/dt$ in the following section.

3. Description of the solar and interplanetary triggers of the events

3.1. Event on May 15, 2005

The first event of Table 1 gives the impression of an event that can be easily followed throughout the whole Sun–Earth chain: an M8.0 flare on May 13, 2005, at 16:13 UT related to the eruption of the large sigmoidal structure in NOAA active region 10759, which released the CME observed by LASCO at 17:22 UT. Then, in-situ measurements at L_1 (ACE), Fig. 1, show low temperature, high magnetic field strength and a smooth rotation through a large angle of the magnetic field vector, which are common features of a magnetic cloud (MC) (Burlaga et al., 1981), the interplanetary counterpart of a subset of CMEs. A few hours later, a geomagnetic disturbance appears at the terrestrial environment. These almost 'academic' features along the solar–terrestrial chain have been assumed as the scenario of this event (e.g. Yurchyshyn et al., 2006; Zhang et al., 2007). However, there are three facts that guide Dasso et al. (2009) to consider a different scenario: (1) too high magnetic field strength (higher than 50 nT), far from typical values for magnetic clouds at 1AU, which have enhanced magnetic field strength in the range of 15–30 nT (Lepping et al., 1990); (2) the problems trying to reproduce the magnetic topology with a single magnetic flux rope; and (3) the long duration of the cloud as it passes the spacecraft (1 day and 9 h, considering the boundaries identified by Yurchyshyn et al. (2006) or 16.6 h as identified at http://wind.nasa.gov/mfi/mag_cloud_pub1.html). This long travel time crossing the ACE spacecraft, together with the large velocity (almost 1000 km/s), led these authors to estimate a diameter of 0.8 or 0.5 AU, which are far from the common values expected at 1 AU in the range of 0.2–0.4 AU (Lepping et al., 1990).

The detailed study made by Dasso et al. (2009) provides strong arguments to consider that there are two different eruptions coming from different parts of the same filament, which interact at some place in the interplanetary medium before reaching L_1 point, where they were observed as two attached, but non-merged magnetic clouds (shadowed areas in Fig. 1). Based on type II radio burst features in the kilometer domain, observed by the TNR experiment on WAVES, Dasso et al. (2009) proposed that

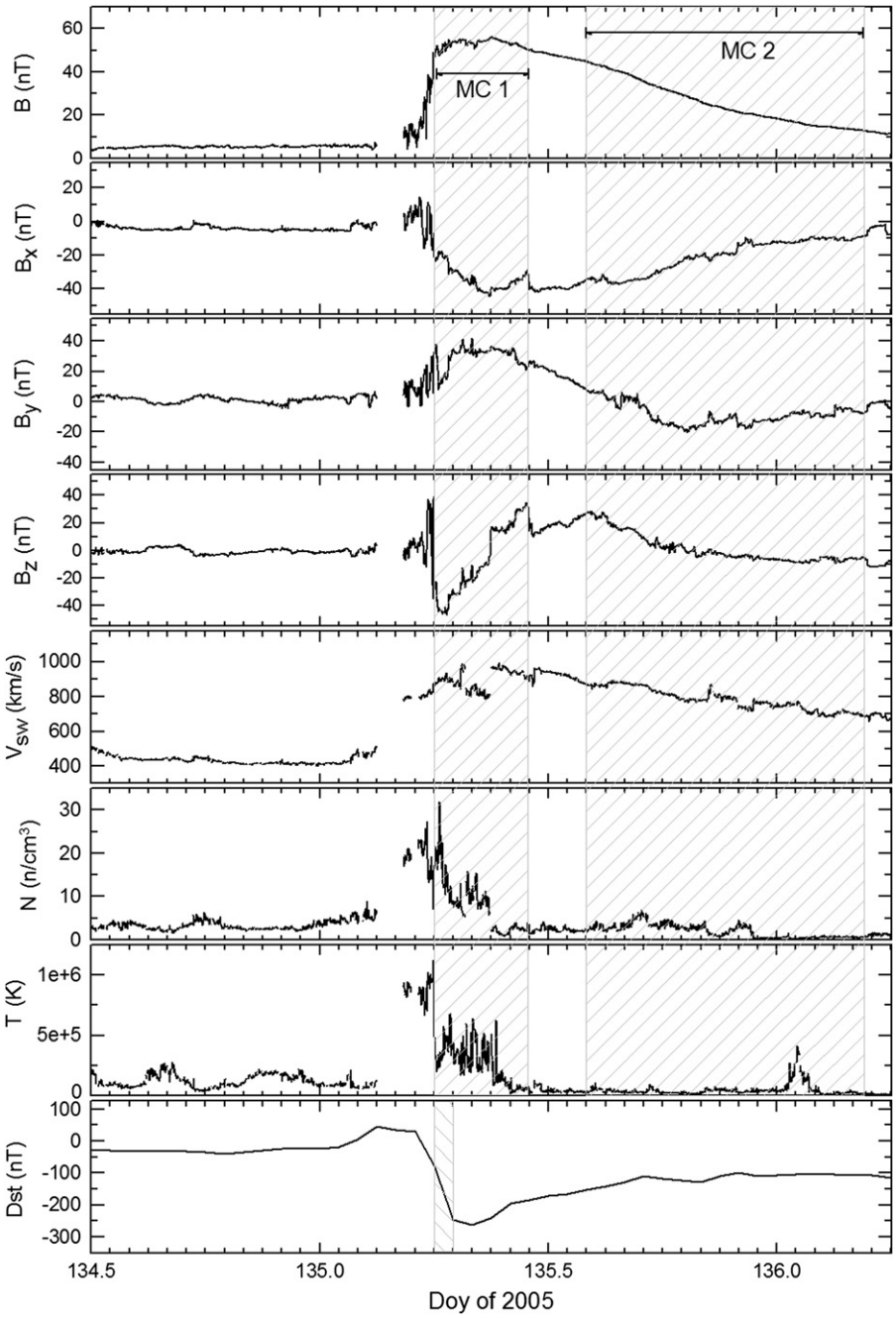

Fig. 1. Interplanetary data and *Dst* index measured for the event on May 15, 2005. From top to bottom are plotted: magnetic field strength and GSM magnetic field components, bulk speed, proton number density and radial component of the proton temperature. The regions indicated by shadowed areas correspond to magnetic clouds, as identified by Dasso et al. (2009). The bottom panel shows the geomagnetic index *Dst*. The shadowed area in this panel indicates the interval of the largest *dDst*/*dt* for this event (see text for detail).

two solar ejections occurred on May 13, 2005, with a difference of about 4 h, both from AR 10759, and with the last ejection traveling faster than the first one (almost twice) and interacting at some place between the Sun and the Earth. As a result, a compression of the first magnetic cloud by the second one might be related to the large magnetic field B_z component, which passes from +37 to −44 nT in less than 40 min (staying below −10 nT for more than 3 h (Gonzalez and Tsurutani, 1987)), with the corresponding enhancement of the geoeffectiveness at the terrestrial environment. On May 15 (doy 135) *dDst*/*dt* was less than −100 nT/h in two successive intervals: between 05 and 06 UT (from +30 to −77 nT) and between 06 and 07 UT (from −77 to −247 nT). The large decrease of *Dst* (277 nT between 05 and 07 UT) could be related to the small magnetic cloud described by Dasso et al. (2009) and the preceding sheath, which is compressed by the second one, resulting in a larger magnetic field strength (Wang et al., 2005; Lugaz et al., 2005).

3.2. Event on November 6, 2001

Solar wind measurements show a complex magnetic structure for the second event of Table 1, November 6, 2001 (Fig. 2). An overlapping shock on November 6 (doy 310) at 01:24 UT (dashed line and "S" in Fig. 2) is a clear indicator of interaction among several solar ejections (Wang et al., 2003a). The compression between this shock and the preceding magnetic cloud (see front

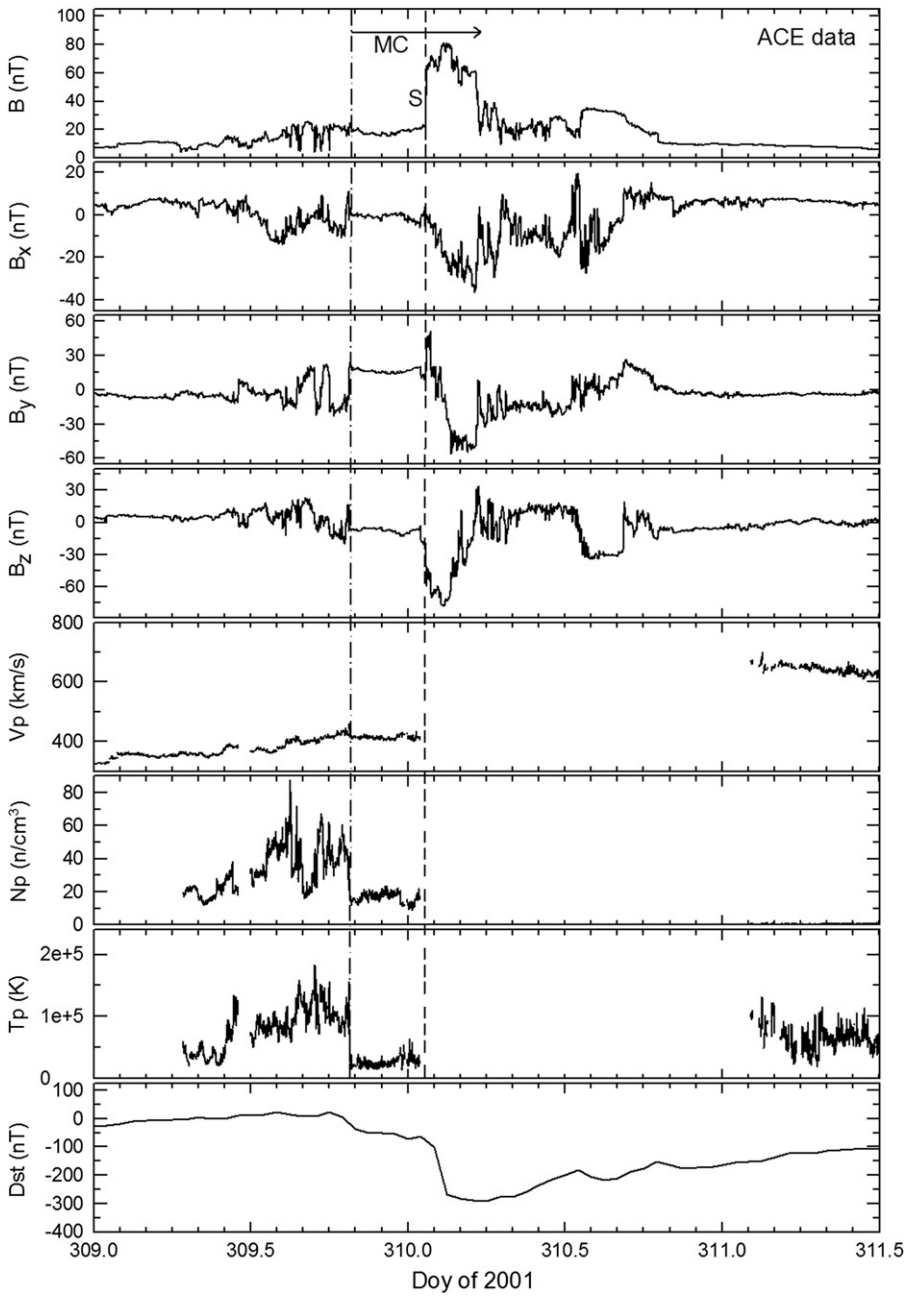

Fig. 2. Interplanetary data and *Dst* index measured for the event on November 6, 2001. From top to bottom are plotted: magnetic field strength and GSM magnetic field components, bulk speed, proton number density and radial component of the proton temperature. Interplanetary data for this Figure comes from ACE Level 2 (verified) Data web site at http://www.srl.caltech.edu/ACE/ASC/level2/ in order to avoid the data gap for magnetic field data for these dates at OMNIweb database. Therefore, solar wind data are not shifted to the Earth Bow Shock Nose. The bottom panel shows the geomagnetic index *Dst*. A first dashed – dotted line indicates the front boundary of a magnetic cloud. An arrow indicates the region of the cloud, which rear boundary cannot be established due to the data gap in solar wind plasma parameters. The dashed line with an "S" indicates the overtaking shock identified by Wang et al. (2003a).

boundary indicated by a dashed–dotted line in Fig. 2) increased the geoeffectiveness triggering the large decrease of *Dst* index from −101 nT on November 6 (doy 310) at 02 UT to −269 nT at 03 UT. Although the Sun was very active on that date, Xie et al. (2006) stated that three full halo CMEs were the solar sources related to this disturbance. They also stated that the event involved a high speed stream. The onset of the first CME at LASCO C2 coronagraph was November 1 at 22:30 UT, whose velocity in the plane of the sky was 453 km/s. An M1.1 flare related to this CME started at GOES at 21:38 UT in N12W23 (active region NOAA 9682). The second CME was observed by LASCO C2 on November 3 at 19:20 UT with a linear fit speed of 457 km/s and related to case an X-class flare from N06W18 (active region NOAA 9684). Finally another full halo was seen by LASCO on November 4 at 16:35 UT associated to an M2.1 class flare from the active region NOAA 9684, as the previous CME, but with a speed of 1810 km/s, about four times the speed of the previous CMEs. As a result, the two first front halo CMEs, from different active regions, but very close in the solar surface, are expected to interact with the last one, increasing in an extraordinary way the magnetic field B_z component until −77 nT, staying below −40 nT for more than 2 h. After that, a large disturbance took place at terrestrial environment as indicated by *Dst* index, that peaked −292 nT after a two-step main phase (Cid et al., 2008). Although the number of peaks in *Dst* is not necessarily directly related to the number of interplanetary transients that are involved in

generating the storm (Richardson and Zhang, 2008), Farrugia et al. (2006) proposed that interacting ejecta are an important interplanetary source of double-dip major storms. Specifically for this event, the main phase starts with the arrival of the magnetic cloud. Then, the second dip in *Dst* index, where *Dst* decreases −168 nT in 1 h, corresponds to the arrival of the overtaking shock on November, 6 (doy 310) at 01:24 UT. The time of the shock arrival corresponds to the shock time at magnetic field data, as there is a large data gap at solar wind data, at Ace and Wind spacecraft. Although this data gap does not provide quantitative density values, they should be large enough to saturate solar wind plasma instruments on board and, as a consequence, to produce a large dip, as proposed by Farrugia et al. (2006) for the event on March 31, 2001. In that event, the major factor determining the intensity of the storm was the very high plasma sheet density, well correlated with the very high solar wind density. Therefore, we can conclude that this overtaking shock, which was also identified by Zhang et al. (2007) as an ICME driven shock propagating through a preceding ICME, was the cause of the large *dDst*/*dt* for this event.

3.3. Event on August 24, 2005

Fig. 3 shows interplanetary data and *Dst* index measured for the period August 23–25, 2005 (doys 235–237) that corresponds to the third event of Table 1. At a first glance the geomagnetic storm seems to be associated with a corotating interaction region (CIR) created by a fast wind interacting with a previous slow wind

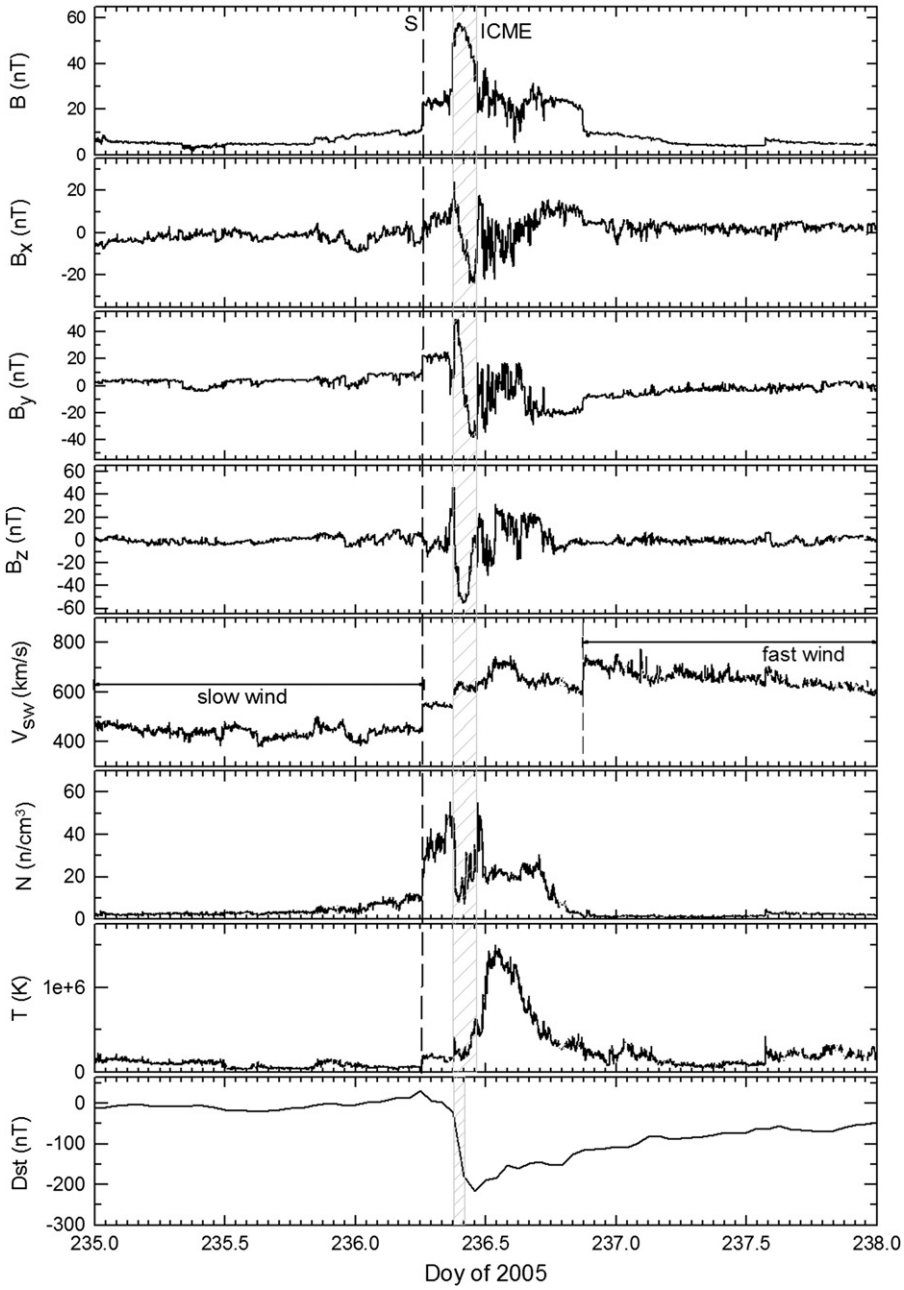

Fig. 3. Interplanetary data and *Dst* index measured for the event on August 24, 2005. From top to bottom are plotted: magnetic field strength and GSM magnetic field components, bulk speed, proton number density and radial component of the proton temperature. The bottom panel shows the geomagnetic index *Dst*. Two regions are indicated in panel 5th corresponding to a slow and a fast wind. A dashed line with an "S" in top panels (solar wind measurements) indicates a shock and shadowed area in these panels corresponds to an ICME (see text for detail). The shadowed area in bottom panel indicates the largest decrease in *Dst* index for the event.

(see fifth panel in Fig. 3). As expected, the region between both winds exhibits a high temperature and a highly fluctuating B_z component. Looking at EIT images (Fig. 4), a coronal hole appears clearly at the solar surface close to the disk center from where the fast stream emanates. However, this kind of interplanetary events is usually related to moderate storms where $-50 > Dst > -100$ nT (Xu et al., 2009; Gonzalez et al., 1999), and the main phases of the resultant magnetic storms typically have irregular profiles. As a result, large hourly variations in *Dst* are not expected for such interplanetary signatures, but small decreases one after another. However, in this case, the *Dst* index decreases from -22 nT on August 24 (doy 236) at 09 UT to -180 nT at 10 UT (shadowed area on bottom panel of Fig. 3). This large variation in *Dst* is associated with a 1 h interval where B_z reaches values below -50 nT, which is not usual inside a CIR, for which field strengths fall typically in the range of 5–15 nT at 1 AU (Zhang et al., 2008). This high magnetic field strength corresponds to a region where B_z can be considered smooth, and the temperature is relatively low. These signatures indicate that the spacecraft is inside an interplanetary coronal mass ejection (ICME), which drives the forward shock on August 24 (doy 236) at 06:10 UT (dashed line and "S" in Fig. 3). Moreover, the clear rotation of the B_x and B_y magnetic field components along with B_z maximum when both *x* and *y* components get zero value indicates that it presents a flux rope structure with its axis pointing along the *z* axis (shadowed area in top panels).

About the solar source of this magnetic cloud, two different M-class flares took place on August 22, 2005, both of them from the active region NOAA 10798. The first one (M2.6), starting at 00:44 UT from S11W54, was related to the CME described above, with a speed of 1194 km/s, and a second one, more intense (M5.6), at 16:46 UT from S13W65 and related to a CME with onset at LASCO C2 at 17:30 UT and with a speed of 2378 km/s. Both of them have been related to this geomagnetic storm by Zhang et al. (2007). However, only one ICME is observed at L1. The assignment of the correct CME to the signatures observed at L1 is out of the scope of this study.

As stated above, the sharp decrease on *Dst* was related to the sharp increase in the B_z component and therefore the question to be addressed is what produced such a high magnetic field strength inside the ICME. A careful analysis of solar wind data for the whole event is necessary for this task. Solar wind density remains above 30 cm^{-3} after the shock until the ICME passage when it decreases sharply until around 10 cm^{-3} and then starts a new increase until around 40 cm^{-3}. Then, between 11:39 and 12:00 UT, the density drops to about 20 cm^{-3} and the temperature increases suddenly from below 5×10^6 K to above 10^7 K. This region corresponds to the stream interface, which separates slow and fast solar wind streams (Burlaga, 1974; Gosling et al., 1978).

An inspection of a time sequence of SOHO EIT 28.4 nm images (Fig. 4) reveals that after the ejection of a halo CME on August 22 at 01:31 UT, the size of a coronal hole close to the central solar meridian increased towards the West, indicating an interaction between the active region NOAA 10798 and the coronal hole mentioned above, which can be guessed from in-situ measurements. As stated above, solar wind temperature and density values increased before the arrival of the stream interface suggesting that the magnetic cloud was compressed by the fast stream. As the coronal hole is close to the solar equator and the magnetic cloud axis follows the *z* direction, the magnetic cloud is expected to be carried away from the Sun by the stream as a small-scale transient caught in the compression region between the two streams, as shown by Rouillard et al. (2009). This kind of interaction between active regions, involving flares and/or filament eruptions, occurring close to growing lowlatitude coronal holes was already associated with intense geomagnetic activity by Gonzalez et al. (1996).

3.4. Event on March 31, 2001

Wang et al. (2003b, 2005) proposed and simulated a structure named multiple-magnetic cloud (Multi-MC) for the signatures observed in the solar wind of the event on March 31, 2001 (number 4 of Table 1). In contrast to complex ejecta, a Multi-MC is formed by a series of successive MCs (or sub-clouds), which satisfy the criteria of a typical magnetic cloud, and interacting regions between them. In this event, two clouds can be easily distinguished in the solar wind data (shadowed regions in Fig. 5), separated by an increase in plasma beta (Wang et al., 2003b). Other ejecta complete the in-situ events. The sub-clouds and ejecta observed in the solar wind are the counterparts of three full halo CMEs on March 28 at 01:27 UT, 12:50 UT and March 29 at 10:26 UT from NOAA 9393, when the active region was passing through the solar central meridian. The increasing velocity of the three CMEs (427, 519 and 942 km/s) let the latter to reach the former ones, with a consequent compression of the magnetic field lines, leading to B_z values of about -50 nT and therefore enhancing their geoeffectiveness. Thus *Dst* decreased from -8 nT on March 31 (doy 90) at 04 UT to -156 nT at 05 UT and to -256 nT at 06 UT, decreasing twice the threshold -100 nT/h. Both

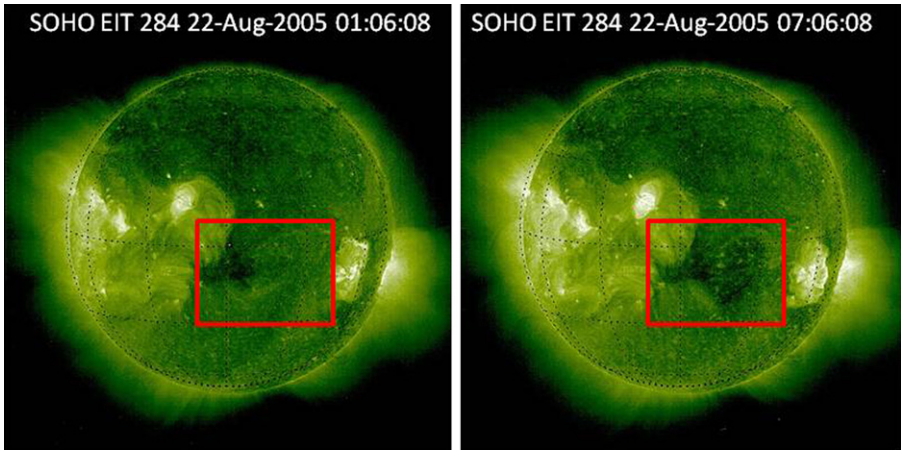

Fig. 4. SOHO EIT images in the Fe XV band pass (284 Å). A coronal hole close to central meridian appears in the images. The ejection of the halo CME on August 22 at 01:31 UT took place from S11W54 between both images. The extension of the coronal hole close to the central solar meridian (marked with a square) increases from the first image to the second one.

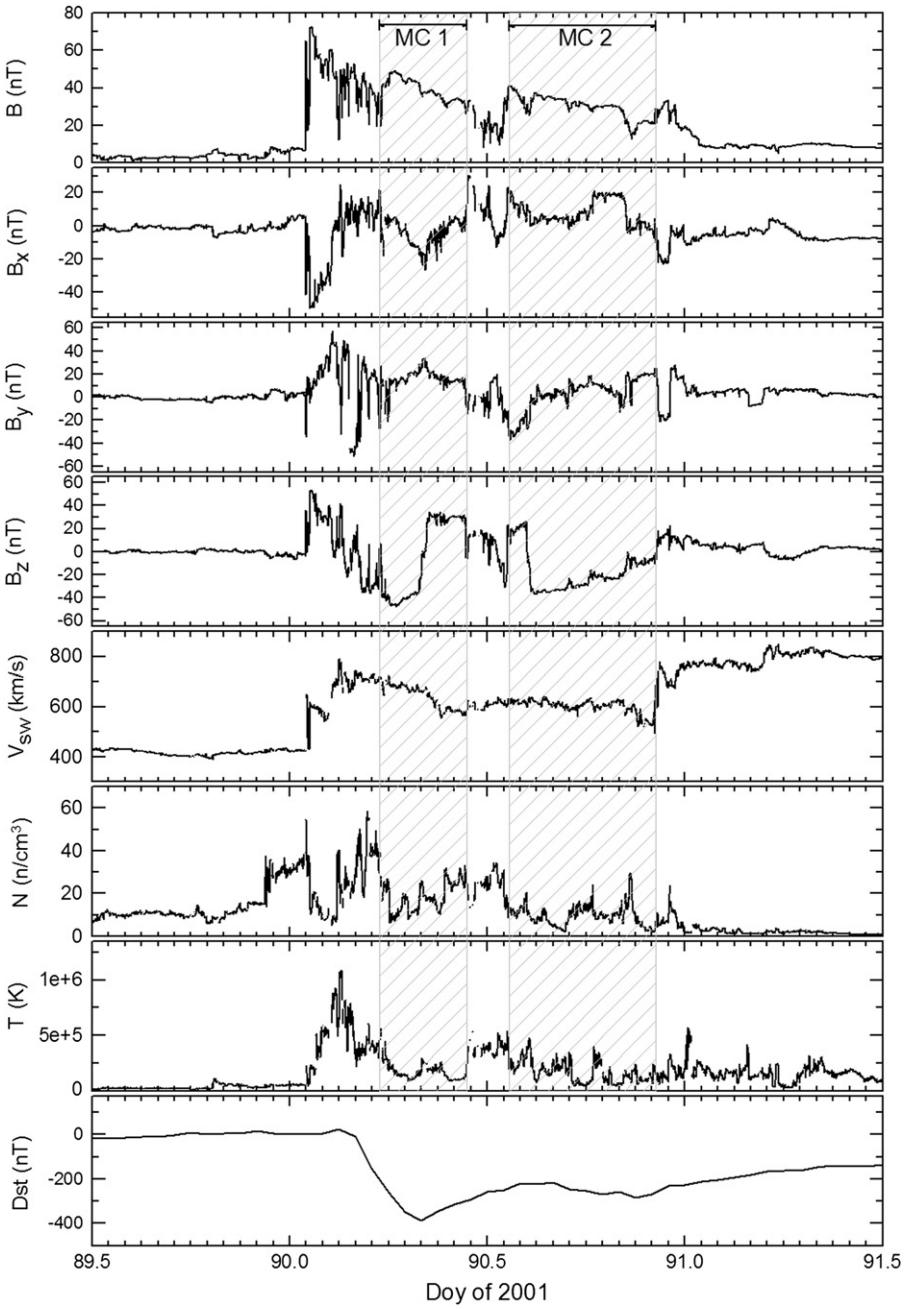

Fig. 5. Interplanetary data and *Dst* index measured for the event on March 31, 2001. From top to bottom are plotted: magnetic field strength and GSM magnetic field components, bulk speed, proton number density and radial component of the proton temperature. The bottom panel shows the geomagnetic index *Dst*. The regions indicated by shadowed areas correspond to magnetic clouds, as identified by Wang et al. (2003b).

decreases are related to the highly fluctuating southern B_z in the sheath field and the interface before the long and large southern B_z of the first sub-cloud.

3.5. Event on July 15, 2000

The event number five of Table 1, also known as the Bastille Day event, has been widely studied by several authors [see as an example a monograph of *Solar Physics* (volume 204, issue 1/2, 2001) devoted to this event]. The full halo CME on July 14, 2000 at 10:54 UT on LASCO C2 coronagraph was associated with a flare observed by EIT from AR9077 at N16.8E0.21 at 10:12UT and with an X5.7 class flare event reported by GOES from this same area starting at 10:03 UT. The solar event and its interplanetary counterpart have been extensively analyzed, but a question should still be solved: what is the cause of the very large interplanetary magnetic field B_z component, which reached −60 nT and kept below −30 nT for more than 1.5 h, making *Dst* to drop from −61 nT on July 15 (doy 197) at 19 UT to −198 nT at 20 UT? Could it be related to the high velocity of the CME (Gonzalez et al., 1998)? Of course this could be an answer; however, a careful inspection of this event reveals similar features to those described above, which could indicate interaction between different solar ejections from the same active region. Several M and X class flares were reported by GOES between July 10 and 14. The three X class flares were related to full or partial halo CMEs on July 11 at 13:27 UT, on July 12 at 11:06 UT and finally on July 14 at 10:54 UT, already mentioned above (other

non-halo CMEs were also observed by LASCO for this period and this active region). The linear fit speed provides for these CMEs the values of 1078, 1124 and 1674 km/s, respectively. Several interplanetary shocks were observed during days 11–15 of July in advance of ICMEs. In total, three shocks driven by three ICMEs were observed by Ace within the four-day interval (doys 195–198) surrounding the Bastille Day event (Smith et al., 2001) (see Fig. 6 where the shocks are shown by dashed lines). After the last of the three shocks (doy 197 at 14:35 UT at OMNIweb data) the temperature increased extraordinarily until 3×10^6 K and the solar wind density increased to approximately 30 cm^{-3} at 15:03 UT. Then, after about 20 min the density values decreased to about 2 cm^{-3} for almost 1 h and increased again to above 20 cm^{-3} at 19:06 UT. The last peak in density corresponds to the large drop in *Dst* and to a highly compressed magnetic field pointing to the south of the ecliptic plane at the rear of the sheath and the beginning of the ICME. These solar wind features fit well with numerical simulations undertaken by Lugaz et al. (2005) where two shocks from two identical CMEs launched in the same direction (the second one 10 h after the first one) merge and a stronger, faster shock appears where the "new" downstream region is hotter. Therefore, the merging of shock waves may have caused a very strong shock in front of the leading ejecta with a compressed magnetic field in the sheath, leading to southern B_z with extreme values. Nevertheless, as shown in Fig. 6, three shocks followed by three ICMEs (corresponding to the three halo CMEs) are observable at 1 AU pointing no merging. Therefore, we cannot be conclusive about the cause for the extraordinarily increased temperature and density and the highly compressed magnetic field observed at solar wind, which could arise as a

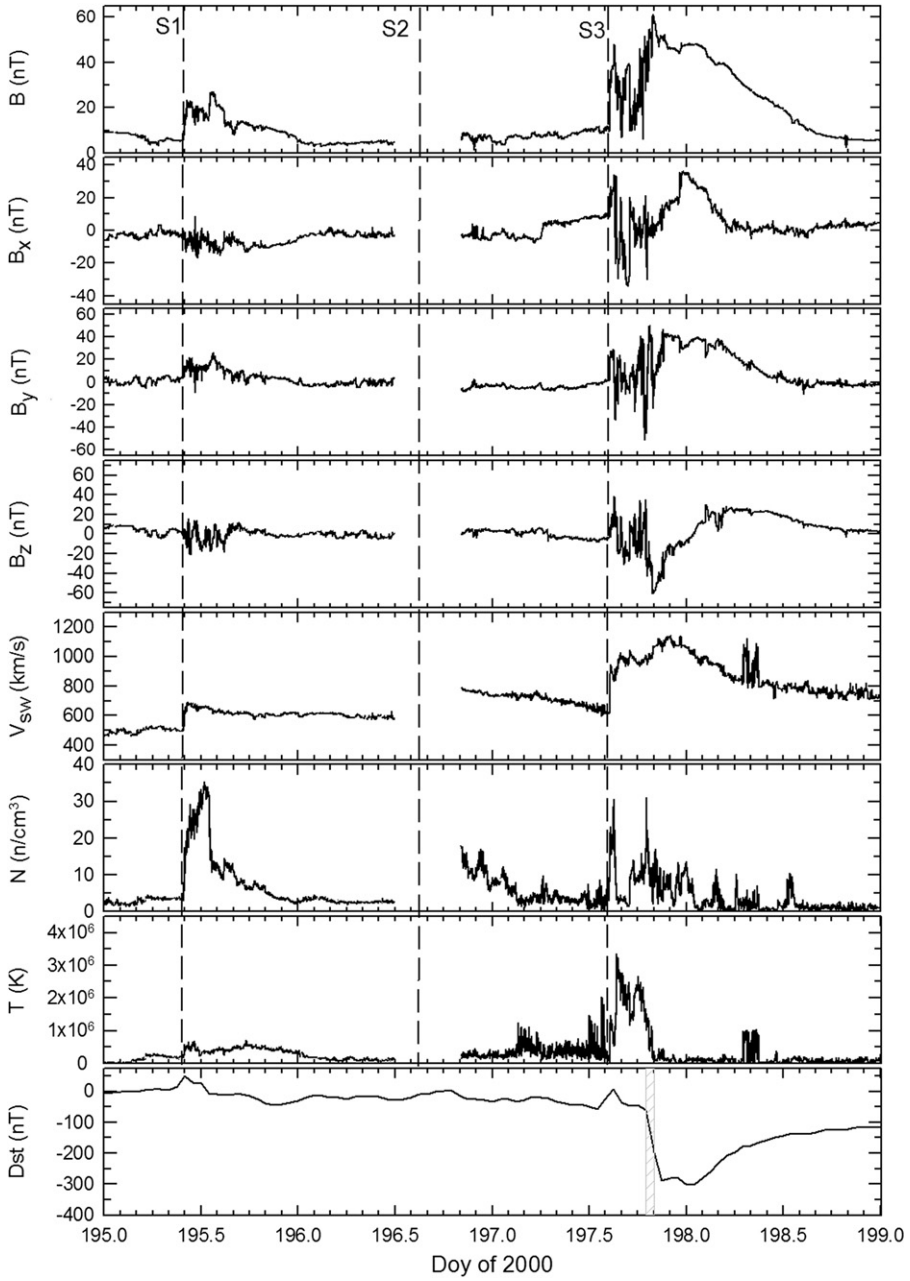

Fig. 6. Interplanetary data and Dst index measured for the event on July 14, 2000. From top to bottom are plotted: magnetic field strength and GSM magnetic field components, bulk speed, proton number density and radial component of the proton temperature. The bottom panel shows the geomagnetic index *Dst*. Dashed lines with "S1", "S2" and "S3" in top panels (solar wind measurements) indicate the three shocks as indicated by Smith et al. (2001). Gap at interplanetary data for this Figure cannot be avoid by using Ace Level 2 (verified) Data, as also contain a data gap. The shadowed area in bottom panel indicates the largest decrease in *Dst* index for the event.

consequence of successive, but non-merged, shock waves. Numerical simulation could help get light on this point, although the enhanced temperature ahead the third shock (S3) already indicates that interaction between this shock and the ICME driving the second shock (S2) exists. This interaction might lead to southern B_z with extreme values because of successive shock waves, as previously indicated for merging shock waves. This large B_z field together with a high solar wind velocity (above 1000 km/s) probably caused the large depression in the *Dst* index (shadowed area in the bottom panel).

3.6. Event on September 17, 2000

Several full and partial halo CMEs from the same active region are also related to the event number 6 (September 17, 2000) of Table 1. Two partial halo CMEs on September 15 at 12:06 and 15:26 UT and two full halo CMEs on September 15 at 21:50 UT and on September 16 at 05:18 UT, all of them related to M class flares from NOAA 9165 active region, have been associated with this geomagnetic storm (Zhang et al., 2007; Burlaga et al., 2001; Xie et al., 2006). As in the previous case the projected speed of the last CME, 1215 km/s, was much larger than the previous ones, with speeds of 633, 481 and 257 km/s. Then, this CME could have overtaken the former ones as it traveled far away from solar surface developing a complex ejecta (Burlaga et al., 2001, 2002). This was observed at in-situ data (shadowed areas in Fig. 7), where at least a sub-cloud and an ejecta can be distinguished. The highly fluctuating magnetic field and solar wind velocity on September 18 (doy 262) could also indicate the interaction of these ejections with material coming from the large coronal holes

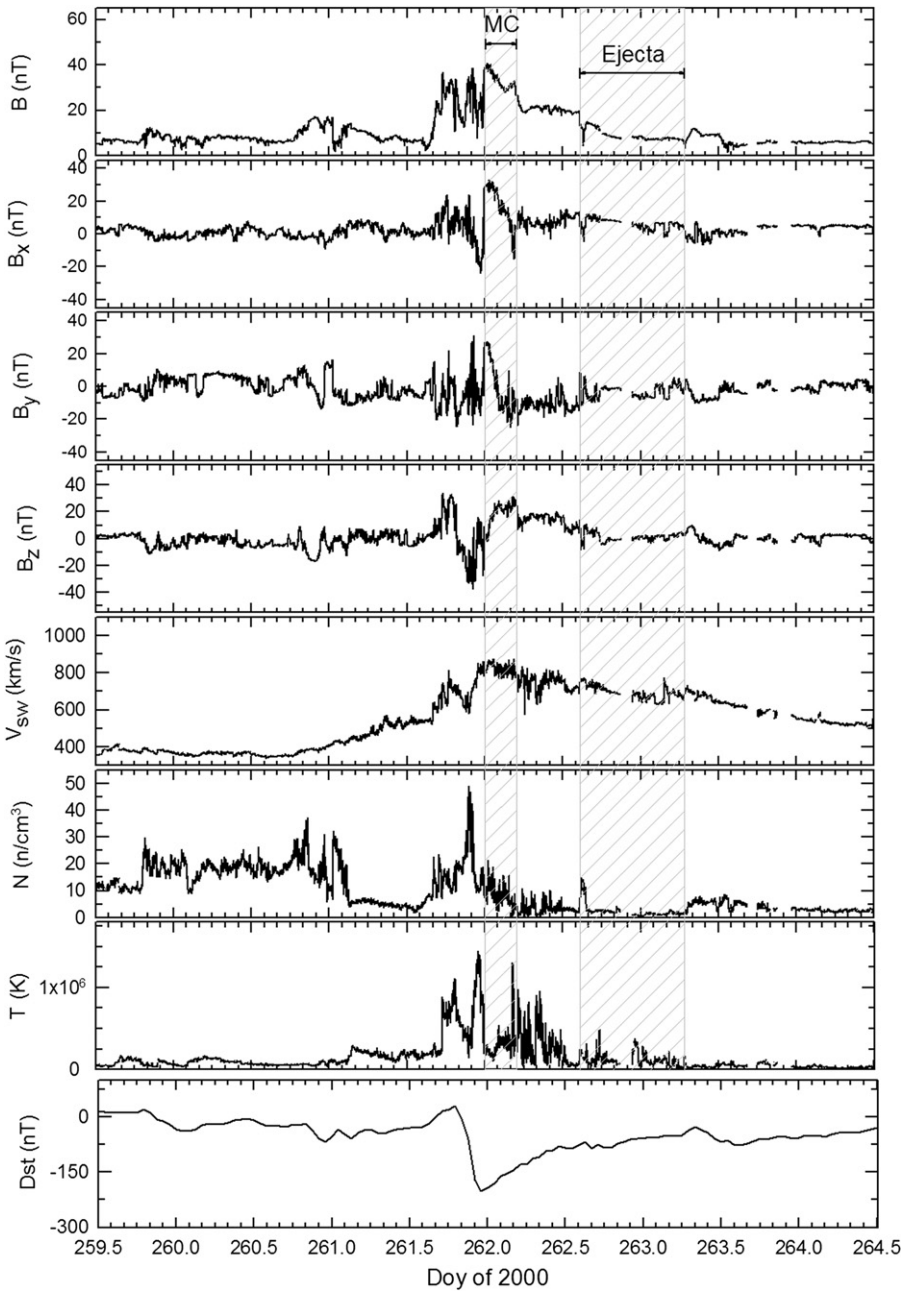

Fig. 7. Interplanetary data and *Dst* index measured for the event on September 17, 2000. From top to bottom are plotted: magnetic field strength and GSM magnetic field components, bulk speed, proton number density and radial component of the proton temperature. The bottom panel shows the geomagnetic index *Dst*. Two regions are indicated with shadowed areas which correspond to a sub-cloud and an ejecta, inside a Multi-MC region.

close to the central solar meridian and next to the active region related to the CMEs. The large hourly *Dst* variation took place between 21 and 22 UT on September 17 (doy 261), when *Dst* dropped from −61 to −171 nT. This decrease in *Dst* can be related to several signatures in solar wind inside the sheath of the complex ejecta: (1) a southern B_z, which reached −37 nT and got values below −10 nT for about 2.5 h, (2) a large increase in solar wind density until above 50 cm^{-3} and (3) an enhancement in temperature over 10^6 K. The arrival of large $B_z<0$ interval (1st signature), together with a high solar wind velocity, could have intensified the ring current. Following Farrugia et al. (2006), we consider that the compression of plasma, as deduced from the enhancement in density and temperature in the sheath, could have also played a key role in the *Dst* drop.

3.7. Event on November 20, 2003

The seventh and the last event from Table 1 (November 20, 2003) present an interval (wider dashed area in Fig. 8) with smooth B_z rotation, enhanced magnetic field strength and relative low temperature, together with a slow decreasing solar wind velocity, which correspond to features of a magnetic cloud. Gopalswamy et al. (2005) has discussed in detail the solar ejection, which could be related to this geomagnetic storm, which was the largest of cycle 23. They associated the November 20 magnetic cloud with the 08:50 UT halo CME (speed in the plane of the sky ~1660 km/s) on November 18 from AR501 at S01E33. However, as stated above for other events as the Bastille one, it is not common for the magnetic field strength in magnetic clouds to

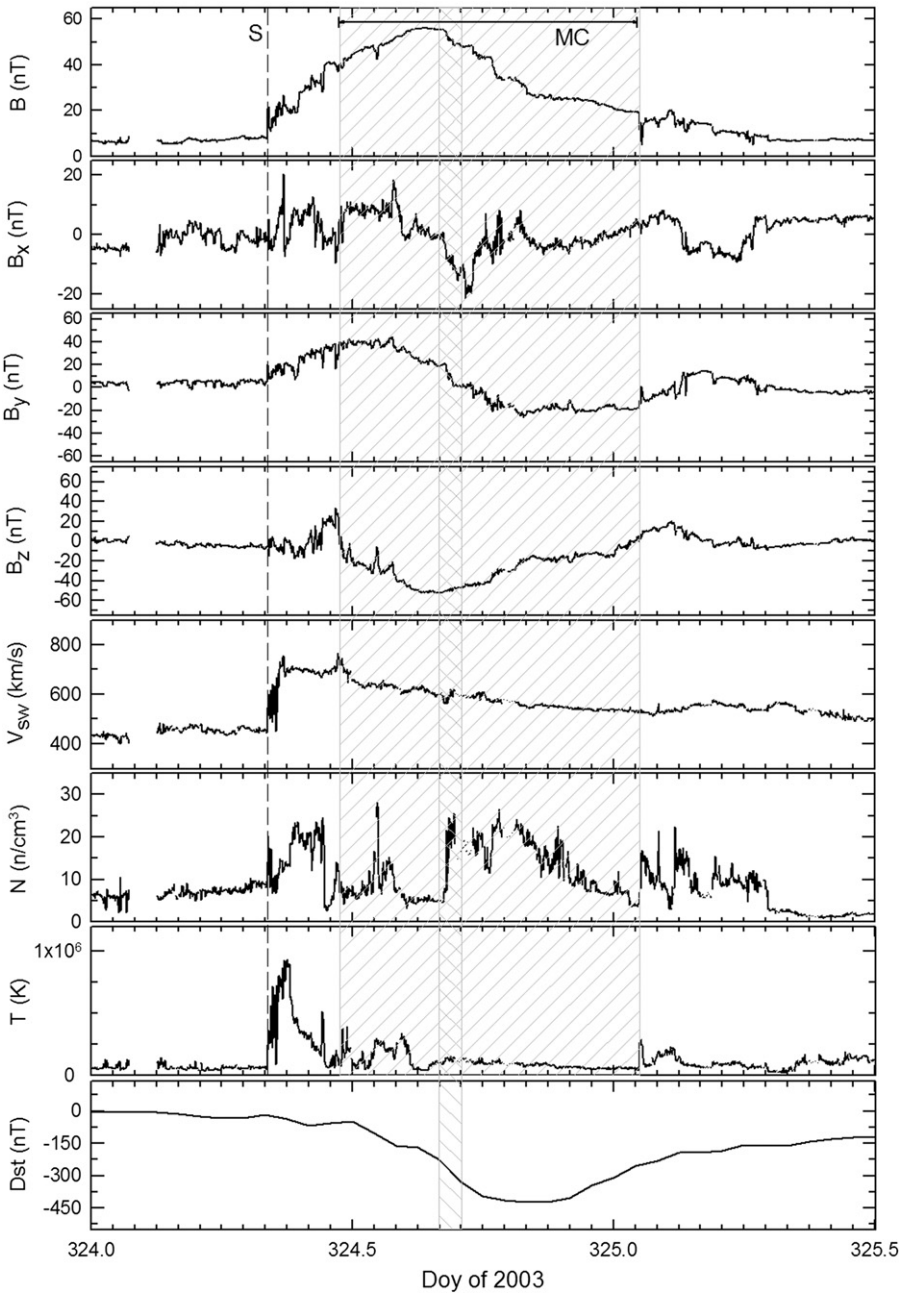

Fig. 8. Interplanetary data and *Dst* index measured for the event on November 20, 2003. From top to bottom are plotted: magnetic field strength and GSM magnetic field components, bulk speed, proton number density and radial component of the proton temperature. Dashed line with an "S" indicates the fast forward shock driving the magnetic cloud (wide shadowed area). The narrow dashed area corresponds to the largest decrease in the *Dst* index.

reach more than 50 nT. Gopalswamy et al. (2005) propose that the extreme field strength of the MC may be due to a combination of two factors: the flux rope originated in an active region instead in a quiescent filament region, and the difference between the MC speed and the upstream speed was relatively large and therefore the MC suffered from a strong front-side compression. However, the large *Dst* drop, which takes place on November 20 (doy 324) between 16 and 17 UT from −229 to −329 nT, cannot be the result of the leading shock (dashed line in Fig. 8) or even the sheath before the MC. During the passage of these solar wind features, and also during the first part of the MC passage, *Dst* decreases more or less smoothly (up to 60 per hour), at the same rate as B_z is more and more southern. However, the largest decrease in *Dst* (100 nT in 1 h), showed as the narrower dashed area in Fig. 8, takes place when southern B_z is increasing and therefore it cannot be related to the extreme field strength of the MC or to the interplanetary shock produced by the difference between the MC speed and the upstream speed.

Gopalswamy et al. (2005) also suggest two additional possibilities: the interaction between the high speed stream of the coronal hole, which might compress the MC, and the interaction with another CME from the same region at 08:06 UT (speed in the plane of the sky ∼1223 km/s, width ∼104°). After a careful revision of the event looking at EIT images, we cannot appreciate any change in the size of the coronal hole close to AR501 on November 18, although there are noticeable changes in the size of that coronal hole the day before related to a previous partial halo CME, which appears on LASCO C2 field of view on November 17 at 09:26 UT. About the interaction with a previous CME, that possibility should be kept on mind in the analysis of solar wind data, but we think that the MC seen at 1 AU is only related to the CME observed at 08:50 UT related to the M3.9 flare at 08:30. In order to explain the previous statement, it is necessary to combine solar observations and solar wind data keeping in mind that the flux rope magnetic structure observed in situ must agree on the sign of the magnetic helicity of the solar region from which it originates. As Gopalswamy et al. (2005) state, the ACE data show that the magnetic field in the MC rotates smoothly with an east–south–west chirality. Yurchyshyn et al. (2005) estimated the AR501 helicity as positive, in agreement with that of the MC. However, Möstl et al. (2008) discussed that concluding that the handedness (or helicity sign) of the very extended filament was ambiguous. Chandra et al. (2009) conclude that the large scale magnetic field of the AR501 has a negative sign, contradicting what is expected from magnetic helicity conservation. However, Chandra et al. (2009) also show the existence of a localized flux of positive helicity in the southern part of AR501 and conclude that during the M3.9/2N flare at 08:30 UT (associated with the halo CME related to the MC) two segments of the filament with opposite chilarities interacted through magnetic reconnection and the helicity carried by both segments partially canceled, transporting away a net-positive helicity, as measured by ACE at 1 AU.

The fact that the interaction between the flux ropes took place at the Sun instead at the interplanetary medium could explain the smooth rotation of the magnetic field, far away from the ejecta or Multi-MC features. However, there are some remaining signatures of this interaction such as the unusual high solar wind density (above 20 cm^{-3}) observed in the magnetic cloud (starting at double dashed area). Specifically, proton density increased on November 20 (doy 324) from approximately 5 cm^{-3} to more than 20 cm^{-3} in less than 10 min (from 16:12 to 16:20 UT), although this increase is not too high when compared with the value at the preceding shock and sheath (corresponding to a MC). The temperature is also enhanced by a factor larger than 2 (from below 5×10^4 K before 15:31 UT of doy 324 to above 10^5 K after 15:43 UT) being even higher than solar wind temperature before the forward shock.

Farrugia et al. (2006), using a kinetic model to simulate the temporal behavior of the ring current buildup during the passage of an ejecta merger, show that the strength of the ring current depends essentially on two factors: the convection electric field in which particles drift and the seed density population. Using as a case the two-step storm on March 31, 2001, they show that the hot dense plasma sheet was of solar origin, in agreement with a previous result by Borovsky (1998), concluding that the major factor determining the severity of that storm was the enhanced plasma sheet density. As the large decrease on the *Dst* index (−100 nT) takes place between 16 and 17 UT when the density increases sharply, we conclude that the interaction between the two segments of the filament with opposite chilarities are the cause of the large variation on the *Dst* for this event.

4. Summary and conclusions

In this paper we have searched for the solar sources and related interplanetary structures that could have been associated with the seven largest *Dst* index decreases ($dDst/dt \leq -100$ nT/h) that took place along solar cycle 23. Such large and fast $dDst/dt$ should have important role in triggering large GIC events, as discussed in the Introduction.

M or X class flares were always involved in the solar sources that caused the large disturbance at terrestrial surface. Also at least one full halo CME, with a speed on the plane of sky above 900 km/s, participated in every studied event, and two or more successive full or partial halo CMEs were involved in five out of the seven events. An increase in the event geoeffectiveness associated with successive halo CMEs has been proposed by Gopalswamy (2007), considering as indicator the minimum value reached by *Dst*. Our results do seem to support such a proposal.

Concerning the interplanetary medium signatures, all events present a large southern B_z component, ranging between −37 and −77 nT. This high value takes place near or at a sheath/MC interface and is frequently associated with shock compression. The intensification in the $-B_z$ field can also be associated with a complex interaction/compression between consecutive CMEs, as demonstrated by Wang et al. (2005), Lugaz et al. (2005, 2007) or Wu et al. (2002), which carried out MHD simulations of the interaction of two CMEs in the heliosphere. Both simulations reach different scenarios. The simulation by Wu et al. (2002) obtains a cannibalization between CMEs due to magnetic reconnection near the Sun, where two CMEs merge, as might have occurred in event #7, with just one MC appearing in the interplanetary data. On the other hand, Wang et al. (2005) and Lugaz et al. (2005) present a double-MC formation (e.g. event #4) due the interaction taking place in the interplanetary medium, where the process of merging becomes very slow due to the larger scale lengths and lower densities relative to the proximities of the Sun. However, not only interactions between successive CMEs but also the encounter between a high speed stream and a CME could also compress B_z and enhance the event geoeffectiveness. Such interaction between MCs and high-speed streams was addressed by Dal Lago et al. (2001) for three magnetic clouds. Event #3 could be related to this latter scenario.

Interaction between segments of a filament at the solar surface could be the cause of an unusual high solar wind density and temperature inside a smooth magnetic field observed for the event on November 20, 2003 (event #7). Large density and temperature enhancements in the sheath could have triggered the large $dDst/dt$ for the event on September 17, 2000, but in this case the interaction appears in the form of an ejecta instead of a

smooth magnetic field of an MC. In the other cases, successive MCs appear at the interplanetary medium interacting between them, such as the events of May 15, 2005, and March 31, 2001. In the events of November 6, 2001, and July 14, 2000, shocks appear to play a major role in overtaking or compressing ICMEs. However, this type of interaction is not exclusive of CMEs or their driven shock waves. During the event on August 24, 2005, an MC is caught between two streams triggering the large decrease in *Dst* index.

Although not analyzed in this paper due to a lower *dDst*/*dt* threshold, the event on January 21, 2005, already mentioned above, is also an interesting event similar to those discussed above although the storm is not so intense ($Dst_{peak}-105$ nT). As indicated by Du et al. (2008), an unusual double-discontinuity characterized by a non-compressive density enhancement, together with an increase in the southward IMF in the solar wind following the discontinuity led to the initial growth of the main phase of this storm. Then, a large *dDst*/*dt* decrease took place during northward IMF, together with a large enhancement in the solar wind density as a result of the interaction between the MC structure and the stream seen in interplanetary data. Such large density enhancement could have played a key role in the large *Dst* decrease, as in the event on August 24, 2005.

From the discussed possible solar/interplanetary causes of the large and fast *Dst* decreases observed in the seven events of this paper, as listed in column 7 of Table 1, one practically common feature was the presence of a compression process occurring at the sheath field region of ICMEs due to one or more subsequent magnetic clouds leading to an interesting and very geoeffective interface/discontinuity that deserves a closer future study.

A systematic study using SYM-H index will also follow in the near future in order to get light about how the temporal resolution used to compute the time derivative of the magnetic field horizontal component (that is, hourly resolution limited using *Dst* data) might impact the study.

Acknowledgments

This work has been supported by Grants: AYA2009-08662, BES-2007-16384 from the Ministerio de Ciencia e Innovación and PPII1001837802 from the Junta de Comunidades de CastillaLa Mancha of Spain. CME information is from the CME catalog generated and maintained by the Centre for Solar Physics and Space Weather, the Catholic University of America, in cooperation with NRL and NASA. SOHO is a project of international cooperation between ESA and NASA. We acknowledge the use of flare events from the National Geophysical Data Center, solar wind magnetic field and plasma data from OMNIweb database, and *Dst* index from World Data Center for Geomagnetism.

References

Belov, A.V., Gaidash, S.P., Eroshenko, E.A., Lobkov, S.L., Pirjola, R., Trichtchenko, L., 2007. Effects of strong geomagnetic storms on Northern railways in Russia. In: Proceedings of the 7th International Symposium on Electromagnetic Compatibility and Electromagnetic Ecology, Saint-Petersburg, Russia, 26–29 June 2007, pp. 280–282.

Borovsky, J., 1998. Lightning energetics: Estimates of energy dissipation in channels, channel radii, and channel-heating risetimes. J. Geophys. Res. 103 (D10), 11537–11553.

Burlaga, L., 1974. Interplanetary stream interfaces. J. Geophys. Res. 79 (25), 3717–3725.

Burlaga, L.F., Sittler, E., Mariani, F., Schwenn, R., 1981. Magnetic loop behind an interplanetary shock: Voyager, Helios, and IMP 8 observations. J. Geophys. Res. 86, 6673–6684.

Burlaga, L.F., Skoug, R.M., Smith, C.W., Webb, D.F., Zurbuchen, T.H., Reinard, A., 2001. Fast ejecta during the ascending phase of solar cycle 23: Ace observations, 1998–1999. J. Geophys. Res. 106 (A10), 20957–20977.

Burlaga, L.F., Plunkett, S.P., Cyr St., O.C., 2002. Successive CMEs and complex ejecta. J. Geophys. Res. 107 (A10), 1266. doi:10.1029/2001JA000255.

Cid, C., Saiz, E., Cerrato, Y., 2008. Comment on "Interplanetary conditions leading to superintense geomagnetic storms ($Dst \leq -250$ nT) during solar cycle 23" by E. Echer et al. Geophys. Res. Lett. 35, L21107. doi:10.1029/2008GL034731.

Cid, C., Hidalgo, M.A., Saiz, E., Cerrato, Y., Sequeiros, J., 2004. Sources of intense geomagnetic storms over the rise of solar cycle 23. Sol. Phys. 223, 231–243.

Chandra, R., Pariat, E., Schmieder, B., Mandrini, C., Uddin, W., 2009. How can a negative magnetic helicity active region generate a positive helicity magnetic cloud? Solar Phys. 261 (1), 127–148 26.

Dal Lago, A., Gonzalez, W.D., de Gonzalez, A.L.C., Vieira, L.E.A., 2001. Compression of magnetic clouds in interplanetary space and increase in their geoefectiveness, J. Atmos. Sol.–Terr. Phys. 63, 451–455.

Dasso, S., et al., 2009. Linking two consecutive nonmerging magnetic clouds with their solar sources. J. Geophys. Res. 114, A02109. doi:10.1029/2008JA013102.

Du, A.M., Tsurutani, B.T., Sun, W., 2008. Anomalous geomagnetic storm of 21–22 January 2005: a storm main phase during northward IMFs. J. Geophys. Res. 113, A10214. doi:10.1029/2008JA013284.

Echer, E., Gonzalez, W.D., Tsurutani, B.T., 2008a. Interplanetary conditions leading to superintense geomagnetic storms ($Dst \leq -250$ nT) during solar cycle 23. Geophys. Res. Lett. 35, L06S03. doi:10.1029/2007GL031755.

Echer, E., Gonzalez, W.D., Tsurutani, B.T., Gonzalez, A.L.C., 2008b. Interplanetary conditions causing intense geomagnetic storms ($Dst \leq -100$ nT) during solar cycle 23 (1996–2006). J. Geophys. Res. 113, A05221. doi:10.1029/2007JA012744.

Eroshenko, E.A., Belov, A.V., Boteler, D., Gaidash, S.P., Lobkov, S.L., Pirjola, R., Trichtchenko, L., 2010. Effects of strong geomagnetic storms on Northern railways in Russia. Advances in Space Research 46 (9), 1102–1110. doi:10.1016/j.asr.2010.05.017.

Farrugia, C.J., Jordanova, V.K., Thomsen, M.F., Lu, G., Cowley, S.W.H., Ogilvie, K.W., 2006. A twoejecta event associated with a twostep geomagnetic storm. J. Geophys. Res. 111, A11104. doi:10.1029/2006JA011893.

Gonzalez, W.D., Echer, E., Clua-Gonzalez, A.L., Tsurutani, B.T., 2007. Interplanetary origin of intense geomagnetic storms ($Dst < -100$ nT) during solar cycle 23. Geophys. Res. Lett. 34, L06101. doi:10.1029/2006GL028879.

Gonzalez, W.D., Tsurutani, B.T., 1987. Criteria of interplanetary parameters causing intense magnetic storms ($Dst < -100$ nT). Planet. Space Sci. 35, 1101–1109.

Gonzalez, W.D., Tsurutani, B.T., Gonzalez, A.L.C., 1999. Interplanetary origin of geomagnetic storms. Space Sci. Rev. 88, 529–562. doi:10.1023/A:1005160129098.

Gonzalez, W.D., de Gonzalez, A.L.C., Dal Lago, A., Tsurutani, B.T., Arballo, J.K., Lakhina, G.K., Buti, B., Ho, C.M., Wu, S..T., 1998. Magnetic cloud field intensities and solar wind velocities. Geophys. Res. Lett. 25 (7), 963–966.

Gonzalez, W.D., Tsurutani, B.T., McIntosh, P.S., Clúa de Gonzalez, A.L., 1996. Coronal holeactive regioncurrent sheet (CHARCS) association with intense interplanetary and geomagnetic activity. Geophys. Res. Lett. 23 (19), 2577–2580.

Gonzalez, W.D., Joselyn, J.A., Kamide, Y., Kroehl, H.W., Rostoker, G., Tsurutani, B.T., Vasyliunas, V.M., 1994. What is a geomagnetic storm? J. Geophys. Res. 99 (A4), 5771–5792.

Gopalswamy, N., Yashiro, S., Akiyama, S., 2007. Geoeffectiveness of halo coronal mass ejections. J. Geophys. Res. 112, A06112. doi:10.1029/2006JA012149.

Gopalswamy, N., Yashiro, S., Michalek, G., Xie, H., Lepping, R.P., Howard, R.A., 2005. Solar source of the largest geomagnetic storm of cycle 23. Geophys. Res. Lett. 32, L12S09. doi:10.1029/2004GL021639.

Gosling, J., Asbridge, J., Bame, S., Feldman, W., 1978. Solar wind stream interfaces. J. Geophys. Res. 83 (A4), 1401–1412.

Huttunen, K.E.J., Schwenn, R., Bothmer, V., Koskinen, H.E.J., 2005. Properties and geoeffectiveness of magnetic clouds in the rising, maximum and early declining phases of solar cycle 23. Ann. Geophys. 23, 625–641.

Koen, J., and Gaunt, C.T., 2002. Geomagnetically induced currents at mid-latitudes. In: Proceedings of the 27th General Assembly of the International Union of Radio Science, Maastrich, the Netherlands, 17–24 August 2002, pp. 1–4.

Lario, D., Aran, A., Decker, R.B., 2008. Major solar energetic particle events of solar cycles 22 and 23: Intensities above the streaming limit. Space Weather 6 (S12001), 1–25. doi:10.1029/2008SW000403.

Lepping, R.P., Jones, J.A., Burlaga, L.F., 1990. Magnetic field structure of interplanetary magnetic clouds at 1 AU. J. Geophys. Res. 95 (A8), 11957–11965. doi:10.1029/JA095iA08p11957.

Lugaz, N., Manchester IV, W.B., Roussev, I.I., Tóth, G., Gombosi, T.I., 2007. Numerical investigation of the homologous coronal mass ejection events from active region 9236. ApJ. 659, 788–800. doi:10.1086/512005.

Lugaz, N., Manchester IV, W.B., Gombosi, T.I., 2005. Numerical simulation of the interaction of two coronal mass ejections from Sun to Earth. ApJ 634, 651–662. doi:10.1086/491782.

Möstl, C., Miklenic, C., Farrugia, C.J., Temmer, M., Veronig, A., Galvin, A.B., Vršnak, B., Biernat, H.K., 2008. Two-spacecraft reconstruction of a magnetic cloud and comparison to its solar source. Ann. Geophys. 26, 3139–3152.

Saiz, E., Cid, C., Cerrato, Y., 2008. Forecasting intense geomagnetic activity using interplanetary magnetic field data. Ann. Geophys. 26, 3989–3998.

Richardson, I.G., Zhang, J., 2008. Multiplestep geomagnetic storms and their interplanetary drivers. Geophys. Res. Lett. 35, L06S07. doi:10.1029/2007GL032025.

Rouillard, A.P., et al., 2009. A solar storm observed from the Sun to Venus using the STEREO, Venus Express, and MESSENGER spacecraft. J. Geophys. Res. 114, A07106. doi:10.1029/2008JA014034.

Smith, et al., 2001. Ace observations of the Bastille day 2000 interplanetary disturbances. Sol. Phys. 204 (Numbers 1–2), 227–252. doi:10.1023/A:1014265108171.

Vodyannikov, V.V., Gordienko, G.I., Nechaev, S.A., Sokolova, O.I., Yu., S., Khomutov, Yakovets, A.F., 2006. Geomagnetically induced currents in power lines according to data on geomagnetic variations. Geomagn. Aeronomy 46 (6), 809–813. doi:10.1134/S0016793206060168.

Wang, R., 2007. Large geomagnetic storms of extreme solar event periods in solar cycle 23. Adv. Space Res. 40, 1835–1841.

Wang, Y., Zheng, H., Wang, S., Ye, P., 2005. MHD simulation of the formation and propagation of multiple magnetic clouds in the heliosphere. A&A 434, 309–316. doi:10.1051/0004-6361:20041423.

Wang, Y.M., Ye, P.Z., Wang, S., Xue, X.H., 2003a. An interplanetary cause of large geomagnetic storms: fast forward shock overtaking preceding magnetic cloud. Geophys. Res. Lett. 30 (13), 1700. doi:10.1029/2002GL016861.

Wang, Y.M., Ye, P.Z., Wang, S., 2003b. Multiple magnetic clouds: several examples during March–April 2001. J. Geophys. Res. 108 (A10), 1370. doi:10.1029/2003JA009850.

Wu, S.T., Wang, A.H., Gopalswamy, N., 2002. MHD modelling of CME and CME interactions in a bi-modal solar wind: a preliminary analysis of the 20 January 2001 two CMEs interaction event. In: Sawaya-Lacoste., H., SP-505., E.S.A. (Eds.), SOLMAG 2002. Proceedings of the Magnetic Coupling of the Solar Atmosphere Euroconference and IAU Colloquium 188, 11–15 June 2002, Santorini, Greece, ESA Publications Division, Noordwijk, Netherlands, ISBN: 92-9092-815-8, pp. 227–230.

Xie, H., Gopalswamy, N., Manoharan, P.K., Lara, A., Yashiro, S., Lepri, S.T., 2006. Long-lived geomagnetic storms and coronal mass ejections. J. Geophys. Res. 111, A01103. doi:10.1029/2005JA011287.

Xu, D., Chen, T., Zhang, X.X., Liu, Z., 2009. Statistical relationship between solar wind conditions and geomagnetic storms in 1998–2008. Planet. Space Sci., 57. doi:10.1016/j.pss.2009.07.015.

Yurchyshyn, V., Hu, Q., Abramenko, V., 2005. Structure of magnetic fields in NOAA active regions 0486 and 0501 and in the associated interplanetary ejecta. Space Weather 3, S08C02. doi:10.1029/2004SW000124.

Yurchyshyn, V., Liu, C., Abramenko, V., Krall, J., 2006. The May 13, 2005 eruption: observations, data analysis and interpretation. Sol. Phys. 239, 317–335. doi:10.1007/s11207-006-0177-3.

Zhang, J., et al., 2007. Solar and interplanetary sources of major geomagnetic storms ($Dst \leq -100$ nT) during 1996–2005. J. Geophys. Res. 112, A10102. doi:10.1029/2007JA012321.

Zhang, Y., Sun, W., Feng, X.S., Deehr, C.S., Fry, C.D., Dryer, M., 2008. Statistical analysis of corotating interaction regions and their geoeffectiveness during solar cycle 23. J. Geophys. Res. 113, A08106. doi:10.1029/2008JA013095.